HHS Public Access

Author manuscript

Nat Med. Author manuscript; available in PMC 2009 August 01.

Published in final edited form as:

Nat Med. 2009 February ; 15(2): 169–176. doi:10.1038/nm.1918.

Regulation of cardiovascular development and integrity by the Heart of Glass-Cerebral Cavernous Malformation pathway

Benjamin Kleaveland[1], **Xiangjian Zheng**[1], **Jian J. Liu**[2], **Yannick Blum**[3], **Jennifer J. Tung**[4], **Zhiying Zou**[1], **Mei Chen**[1], **Lili Guo**[1], **Min-min Lu**[1], **Diane Zhou**[1], **Jan Kitajewski**[4], **Markus Affolter**[3], **Mark H. Ginsberg**[2], and **Mark L. Kahn**[1]

[1]Department of Medicine and Cardiovascular Institute, University of Pennsylvania, 421 Curie Blvd, Philadelphia PA 19104 [2]Department of Medicine, University of California San Diego, 9500 Gilman Drive, MC 0726, La Jolla, CA 92093-0726 [3]Biozentrum, University of Basel, Klingelbergstrasse 50/70, CH-4056 Basel, Switzerland [4]Department of Pathology and Department of Obstetrics and Gynecology, Institute of Cancer Genetics and Herbert Irving Comprehensive Cancer Center, Columbia University Medical Center, New York NY 10032

Abstract

Cerebral cavernous malformations (CCMs) are human vascular malformations caused by mutations in three genes of unknown function, *KRIT1, CCM2* and *PDCD10*. Here we show that the HEG1 receptor, linked to *CCM* genes in zebrafish, is selectively expressed in endothelial cells and that *Heg1*$^{-/-}$ mice exhibit defective integrity of the heart, blood vessels and lymphatic vessels. In contrast, *Heg1*$^{-/-}$;*Ccm2*$^{+/lacZ}$ and *Ccm2*$^{lacZ/lacZ}$ mice die early in development due to a failure of nascent endothelial cells to associate into patent vessels, a phenotype shared by deficient zebrafish embryos and reproduced by deficient endothelial cells *ex vivo*. These cardiovascular defects are associated with abnormal endothelial junctions like those observed in human CCMs, and biochemical and cellular imaging studies identify a cell autonomous pathway in which HEG1 receptors couple to KRIT1 at cell junctions. These studies identify HEG1-CCM signaling as a critical regulator of cardiovascular organ formation and integrity.

Introduction

CCMs are a common vascular malformation with a prevalence of 0.1-0.5% in the human population1. CCMs arise primarily in the brain as thin-walled, dilated blood vessels that cause seizures, headaches and stroke in mid-life, often in association with focal hemorrhage1,2. Familial CCMs exhibit an autosomal dominant pattern of inheritance and are caused by loss of function mutations in three genes, *KRIT1* (aka *CCM1*)1,3,4, *CCM2* (aka *MALCALVERNIN* and *OSM*)5,6 or *PDCD10* (aka *CCM3*)7. The CCM proteins are putative adaptor proteins that interact biochemically8-10 and participate in a novel signaling

Correspondence should be addressed to: M.L.K. (markkahn@mail.med.upenn.edu) .

pathway that is not yet fully characterized. How loss of CCM signaling results in the development of vascular malformations is not known.

A clue to the role of CCM signaling in cardiovascular organs has come from genetic studies in zebrafish revealing that loss of *krit1*, *ccm2* or a gene encoding the novel type I transmembrane receptor Heart of Glass (*heg*) results in a dilated heart phenotype early in development11,12. This phenotype is characterized by heart failure associated with enlarged cardiac chambers in which the endocardium is covered by a thin layer of myocardial cells. Expression of *heg, krit1* and *ccm2* mRNAs has been detected in the endocardium but not the myocardium of zebrafish embryos11,12, suggesting that these proteins may operate in an endothelial cell autonomous signaling pathway. An endothelial role for this pathway is also supported by studies of KRIT1-deficient mice that demonstrate lethal vascular defects at E9, but failure to detect high level *CCM* gene expression in the mammalian cardiovascular system has also led to the proposal of cell non-autonomous mechanisms of CCM pathogenesis such as a requirement for CCM signaling in adjacent neuronal cells13.

In the present study we use mice and zebrafish lacking the HEG1 receptor and the CCM2 adaptor to investigate the role of this pathway in the cardiovascular system. Our studies support an endothelial cell autonomous mechanism in which the HEG1 receptor couples to CCM proteins to regulate endothelial cell-cell junctions required for the formation and maintenance of many cardiovascular organs. Complete loss of function in this pathway results in a failure of emerging endothelial cells to associate into a functional cardiovascular system in both the mouse and fish embryo. Less complete loss of function permits formation of cardiovascular organs but results in integrity defects manifest by cardiac rupture, vascular hemorrhage and lymphatic leak. These cardiovascular defects arise in conjunction with abnormal endothelial junctions similar to those observed in human CCMs14-16 and associated with KRIT1 depletion *ex vivo* 17, suggesting a common mechanism by which loss of this signaling pathway confers a spectrum of vertebrate cardiovascular phenotypes in developing and mature animals. Our studies indicate that the pathway implicated in human CCMs regulates endothelial cell-cell association and suggests that agents able to increase endothelial cell association may be effective treatments for CCM.

Results

Heg1 but not *Ccm2* is selectively expressed in the developing cardiovascular system

An outstanding question regarding how loss of CCM proteins confers human vascular disease has been whether and how this pathway functions in cardiovascular cell types. To determine whether HEG1 receptors might play a direct role in regulating CCM signaling we cloned the mouse *Heg1* gene (Supp. Fig. 1) and characterized *Heg1* mRNA expression in mice. In situ hybridization studies demonstrated *Heg1* expression in the endothelium of the developing heart and aorta and in the neural tube at E10.5 (Fig. 1a) and in arterial endothelium and smooth muscle as well as in the endocardium of the heart and brain vasculature at E14.5 (Fig. 1b and Supp. Fig. 2). In contrast to *Heg1, Ccm2* expression appeared low and was detected primarily in the developing neural tube at E10.5 (Supp. Fig. 3).

HEG1-deficiency results in loss of cardiovascular integrity and lethal hemorrhage in mice

To address the role of the HEG1 receptor in mammals, HEG1-deficient mice were generated by targeting *Heg1* exon 1 in embryonic stem cells (Supp. Fig. 4). On both 50% SV129;50% C57Bl/6 and >95% C57Bl/6 backgrounds, HEG1-deficient animals displayed embryonic and post-natal lethality (Supp. Table 1). Mid-gestation HEG1-deficient embryos exhibited cardiac defects characterized by invagination of the ventricular cavity into, and often through, the compact layer of ventricular myocardium (Fig. 1c-f). The septal myocardium was similarly honeycombed by endothelial-lined extensions from the ventricular cavity, a defect accompanied by the presence of ventricular septal defects in most late gestation embryos (Fig. 1g). TUNEL and anti-Ki67 staining revealed that HEG1-deficient myocardial defects were not due to an increase in myocardial apoptosis or a decrease in myocardial proliferation (Supp. Fig. 5 and data not shown). Although most HEG1-deficient animals survived to birth, approximately half died prior to weaning due to pulmonary hemorrhage (Fig. 1g-i). Neonatal HEG1-deficient animals also exhibited defective cardiac integrity manifest by hemopericardium, a phenotype that even arose due to rupture of the low pressure atrial chamber of the heart (Fig. 1j). These findings demonstrate that HEG1-deficiency results in a lethal loss of cardiac and pulmonary vascular integrity.

HEG1-deficient neonates develop chylous ascites due to dilated, leaky mesenteric lymphatic vessels

Neonatal mammals transport absorbed fat through the intestinal and mesenteric lymphatic vessels in the form of white chyle. A distinct phenotype observed in HEG1-deficient neonates was the appearance of chylous ascites shortly after their first feeding (Fig. 2a,b). Chylous ascites was invariably associated with the presence of severely dilated intestinal and mesenteric lymphatic vessels that leaked chyle into the intestinal wall and peritoneal space (Fig. 2c-f). Dilated HEG1-deficient mesenteric lymphatics were lined with endothelial cells that expressed the lymphatic molecular marker LYVE1 and were associated with the smooth muscle cells typical of collecting lymphatics (Fig. 2g,h), but exhibited abnormal endothelial junctions and inter-endothelial cell gaps similar to those observed in human CCMs (Fig. 5). These findings demonstrate that loss of HEG1 receptors is associated with loss of integrity in lymphatic vessels as well as in the heart and blood vessels. Since lymphatic vessels are not subject to hemodynamic forces generated by the beating heart, these findings further suggest that loss of integrity can arise as an intrinsic defect in the cardiovascular organs of HEG1-deficient animals.

Heg1 and *Ccm2* interact genetically in a pathway required for early vessel formation in the mouse

Identical big heart phenotypes arise in zebrafish embryos lacking *heg, krit1 (santa)* or *ccm2 (valentine)*, and co-morpholino experiments demonstrate strong interactions between these genes in the fish12. In contrast, human CCMs have been linked to loss of function mutations in *KRIT1* and *CCM2* but not *HEG1*, and HEG1-deficient mice do not experience the early embryonic lethality reported for KRIT1-deficient mice18. To determine whether and to what extent HEG1 receptors interact with CCM signaling proteins in mammals we intercrossed $Heg1^{+/-}$;$Ccm2^{lacZ/+}$ animals. The $Ccm2^{lacZ}$ allele is predicted to be a null allele because the

Ccm2^{lacZ} mRNA transcript lacks the 3′ half of the *Ccm2* mRNA (exons 6-10, Supp. Fig. 6), and *Ccm2*$^{lacZ/lacZ}$ embryos experience early embryonic lethality that phenocopies *Krit1*$^{-/-}$ embryos (see below and18). In contrast to *Heg1*$^{-/-}$;*Ccm2*$^{+/+}$ animals that exhibit no phenotype prior to midgestation, both *Heg1*$^{-/-}$;*Ccm2*$^{lacZ/+}$ and *Ccm2*$^{lacZ/lacZ}$ embryos died prior to E10 (Supp. Table 2). *Heg1*$^{-/-}$;*Ccm2*$^{lacZ/+}$ and *Ccm2*$^{lacZ/lacZ}$ embryos were indistinguishable from littermates until E9 when they exhibited identical phenotypes of growth retardation and marked pericardial edema despite the presence of a visibly normal heartbeat (data not shown). Histologic examination revealed normal development of the ventricular chamber and bulbis cordis (future right ventricle), but formation of a dilated aortic sac (Fig. 3 and Supp. Fig. 7). In contrast to control embryos, the rostral paired dorsal aortae of E9 *Heg1*$^{-/-}$;*Ccm2*$^{lacZ/+}$ and *Ccm2*$^{lacZ/lacZ}$ embryos appeared small or undetectable and completely lacked luminal blood cells (Fig. 3 and Supp. Fig. 7). Analysis of serial transverse sections revealed that the aortic sac failed to connect to a lumenized first, second or third branchial arch artery in *Heg1*$^{-/-}$;*Ccm2*$^{lacZ/+}$ and *Ccm2*$^{lacZ/lacZ}$ embryos, suggesting that blood in the heart did not enter the dorsal aortae despite the presence of a normal heartbeat (Fig. 3 and Supp. Fig. 7). When visible, the cardinal veins of E9 *Heg1*$^{-/-}$;*Ccm2*$^{lacZ/+}$ and *Ccm2*$^{lacZ/lacZ}$ embryos were also devoid of blood except at the point where they connected to the sinus venosus of the heart (Fig. 3, right panels). In contrast to the lack of blood in the vessels, extravasated blood cells were frequently present in the dilated pericardial cavity (Fig. 3 and data not shown), a finding that may reflect a primary defect in the integrity of the heart like that observed in deficient zebrafish embryos11,12, or may arise secondary to the heart beating against a closed circulatory system and/or reduced embryonic viability at that timepoint.

To determine if the lack of blood-filled vessels in E9 *Heg1*$^{-/-}$;*Ccm2*$^{lacZ/+}$ and *Ccm2*$^{lacZ/lacZ}$ embryos reflects a lack of endothelial cells or their failure to create functional vessels, Flk1 immunostaining was performed to identify endothelial cells. Endothelial cells were found at the appropriate sites for the branchial arch arteries and dorsal aortae, but these cells were not organized into lumenized vessels as in control embryos (Fig. 3). Thus circulation in *Heg1*$^{-/-}$;*Ccm2*$^{lacZ/+}$ and *Ccm2*$^{lacZ/lacZ}$ embryos is blocked by a failure of mutant endothelial cells to form lumenized vessels capable of carrying blood. These findings demonstrate strong genetic interaction between HEG1 receptors and the CCM signaling pathway during formation of the primary vasculature in mammals.

heg and *ccm2* are required for vessel patency but not vessel patterning in zebrafish

In contrast to E9 *Heg1*$^{-/-}$;*Ccm2*$^{lacZ/+}$ and *Ccm2*$^{lacZ/lacZ}$ mouse embryos, zebrafish embryos lacking *heg* and *ccm2* are reported to show primarily cardiac defects11,12. To determine if HEG1 and CCM signaling is utilized in a distinct manner during cardiovascular development in the fish and the mouse we examined vascular patterning and function in *heg* and *ccm2* morphant and mutant zebrafish embryos at 48 hpf. As previously reported, morpholino knockdown of *heg* or *ccm2* in fli1-GFP transgenic fish in which the endothelium is GFP-labeled resulted in dilated heart chambers, but no abnormality in vessel patterning (Fig. 4a). However, we noted visually that blood cells in the hearts of *heg* and *ccm2* morphant fish failed to circulate despite detectable contraction of the dilated heart, a finding similar to the circulatory block observed in E9 *Heg1*$^{-/-}$;*Ccm2*$^{lacZ/+}$ and *Ccm2*$^{lacZ/lacZ}$ mouse

embryos. To functionally test the patency of the vasculature of *heg* and *ccm2* morphant fish we performed angiography. Fluorescent beads injected into the sinus venosus of fish embryos treated with control morpholinos circulated throughout the body and outlined the developing vasculature of the head and tail (Fig. 4b). In contrast, injection of *heg* or *ccm2* morphant fish revealed a complete or nearly complete circulatory block immediately distal to the heart (Fig. 4b), the same point at which circulation is blocked in E9 $Heg1^{-/-};Ccm2^{lacZ/+}$ and $Ccm2^{lacZ/lacZ}$ mouse embryos. A complete circulatory block was also observed in *ccm2* mutant zebrafish embryos using injection of FITC-dextran (Fig. 4c). These findings demonstrate a conserved role for HEG1 and CCM2 in the formation of a patent vertebrate circulatory system.

HEG1-CCM signaling is required for endothelial tube formation but not endothelial cell vacuolization

The failure of nascent endothelial cells to form patent branchial arch vessels in $Heg1^{-/-};Ccm2^{lacZ/+}$ and $Ccm2^{lacZ/lacZ-}$ mouse embryos and *heg* or *ccm2* morphant zebrafish embryos suggested that HEG1-CCM signaling might be required for endothelial cells to form lumenized tubes during early vascular development. To test the role of CCM2 in endothelial tube formation, we examined the ability of human umbilical vein endothelial cells (HUVEC) expressing *CCM2*-specific and scrambled control shRNAs to form tubes using a fibrin bead assay19. *CCM2* shRNA resulted in an 85-90% reduction in CCM2 mRNA expression, and had no effect on endothelial cell size, proliferation or migration (Supp. Fig. 7). Although control HUVEC generated multicellular structures with clearly visible mature lumens at 10 days, CCM2-deficient HUVEC formed branched cords of similar length as control cells but frequently failed to form visible lumens (Supp. Fig. 7).

Studies of lumen formation by endothelial cells *in vitro* and in the intersegmental vessels (ISVs) of the zebrafish embryo *in vivo* have demonstrated that endothelial cells can form lumenized vessels through the formation and fusion of intracellular vacuoles 20-23. We assessed the formation of vacuole-like structures in the ISVs of morphant and control zebrafish embryos using fli1a:EGFP-cdc42 transgenic animals in which GFP-cdc42 fusion proteins outline the intracellular vacuoles that form in endothelial cells22. Endothelial vacuole-like structures formed normally in the ISVs of zebrafish embryos lacking *heg* or *ccm2* (Supp. Fig. 7 and **Supp. Movies** 1-3) and the injection of fluorescent quantum dots into the dorsal aorta of morphant animals (to bypass the block at the level of the branchial arch arteries) confirmed that these vessels formed a patent lumen (Supp. Fig. 7 and **Supp. Movies** 4-6). These findings suggest that defects in endothelial tube formation observed in deficient endothelial cells do not arise due to loss of intracellular endothelial vacuole-like structures.

Loss of HEG1-CCM signaling results in defective endothelial cell junctions in humans, mice and fish

An ultrastructural characteristic of human CCMs is the presence of abnormal endothelial cell-cell junctions and gaps between endothelial cells14-16, and a recent study of KRIT1 function demonstrated a role for that protein in the dynamic regulation of endothelial cell-cell junctions *ex vivo*17. Thus one mechanism by which HEG1-CCM signaling might

regulate cardiovascular organ development and integrity is through regulation of endothelial cell association. To directly assess the role of HEG1 in regulating endothelial junctions *in vivo* we used transmission electron microscopy to examine cell-cell junctions in the endothelium of neonatal mouse lymphatic vessels. The dilated mesenteric lymphatic vessels of *Heg1*$^{-/-}$ neonates exhibited markedly shortened endothelial junctions compared with littermate control vessels (mean length of *Heg1*$^{-/-}$ junctions was 1769 ± 506 nm vs. 3355 ± 1009 nm for *Heg1*$^{+/+}$ junctions, $P = 0.01$, Fig. 5a,b), and were accompanied by endothelial gaps not present in control collecting mesenteric lymphatic vessels (Fig. 5c). Similarly shortened junctions were identified in the endocardium of *ccm2* morphant zebrafish hearts (Supp. Fig. 8). Finally, analysis of the constricted, bloodless aortae of E9 CCM2-deficient mouse embryos also revealed shortened endothelial junctions despite the fact that the caliber of these vessels was markedly reduced (Supp. Fig. 8). These findings indicate that defective endothelial junctions characterize both the dilated and constricted cardiovascular phenotypes of animals lacking HEG1-CCM signaling and are a universal feature of cardiovascular organs lacking this pathway in fish, mice and humans. Significantly, the levels of beta-catenin, VE-cadherin and claudin-5 in HEG1-deficient lymphatic vessels, in the heart and vessels of zebrafish embryos lacking *heg* or *ccm2* and in CCM2-deficient HUVEC were preserved (Supp. Fig. 9). These findings suggest that HEG1-CCM signaling may regulate the function of these proteins rather than their expression.

HEG1 receptors couple to CCM proteins through KRIT1

HEG1 is expressed in endothelial cells in fish and mice, *Heg1*$^{-/-}$ neonates display defects in lymphatic vessels composed primarily of endothelial cells, *Heg1*$^{-/-}$;*Ccm2*$^{lacZ/+}$ and *Ccm2*$^{lacZ/lacZ}$ mouse embryos and *heg/ccm2* morphant zebrafish embryos exhibit aberrant vessel formation at an early developmental timepoint when vessels are composed exclusively of endothelial cells, and CCM2 knockdown HUVEC display tube forming defects. These findings and the detection of heterologously expressed HEG1 at endothelial cell junctions (Supp. Fig. 10) suggested that HEG1 receptors might interact with CCM proteins in a linear, endothelial cell autonomous signaling pathway. To determine whether HEG1 receptors can interact with intracellular CCM2, FLAG-tagged wild type HEG1 receptors and HEG1 receptors lacking most of the intracellular tail (HEG1ΔC) were co-expressed with HA-CCM2 proteins in HEK293T cells, and co-immunoprecipitation experiments performed using anti-FLAG and anti-CCM2 antibodies. CCM2 co-immunoprecipitated with full length HEG1 receptor using either anti-FLAG antibodies to pull down HEG1 or anti-CCM2 antibodies (Fig. 6a,b). In contrast, although truncated HEG1ΔC receptors were expressed at the cell surface at similar levels as full length HEG1 receptors (Supp. Fig. 11), CCM2 failed to co-precipitate with HEG1 receptors lacking the intracellular tail (Fig. 6a,b).

To further define how the HEG1 intracellular tail associates with CCM proteins we used affinity matrices containing the intracellular tail of HEG1 or the aIIb integrin receptor to pull down HA-tagged mouse CCM2 and myc-tagged mouse KRIT1 that were heterologously expressed in HEK293 cells. The HEG1 receptor tail but not that of the aIIb integrin efficiently pulled down KRIT1 and both KRIT1 and CCM2 when they were co-expressed (Fig. 6c). However, only small amounts of CCM2 were pulled down when it was expressed

without KRIT1 co-expression (Fig. 6c), demonstrating that KRIT1 significantly facilitates CCM2 interaction with the HEG1 receptor tail. To further test the mechanism of CCM2 association with HEG1 we compared the ability of HEG1 to interact with krit1 co-expressed with wild type ccm2 or with ccm2L197R, a ccm2 protein with a PTB domain point mutation that blocks binding to KRIT1 8 and has been identified as a cause of human CCM 6. Expression of wild type ccm2 efficiently rescued the big heart phenotype of ccm2-deficient zebrafish embryos but expression of ccm2L197R did not, demonstrating that this point mutation is associated with complete ccm2 loss of function cardiovascular phenotypes in both fish and humans (Supp. Fig. 12). As observed with the mouse proteins, the HEG1 receptor tail efficiently pulled down both krit1 and wild type ccm2 when they were co-expressed, but only krit1 was efficiently pulled down when ccm2L197R was co-expressed (Fig. 6d). Finally, HEG1 receptor tails also efficiently pulled down endogenous KRIT1 despite the fact that the levels of endogenous KRIT1 are so low that it could not be detected in 5% of the input cell lysate by immunoblotting with the same antibody (Fig. 6e). These findings support a model in which HEG1 receptors couple to CCM proteins primarily through interaction with KRIT1 at endothelial cell-cell junctions (Fig. 6f).

Discussion

Human genetic studies have revealed that CCMs arise due to haploinsufficiency of *KRIT1*, *CCM2* and *PDCD10*, and genetic studies in mice and zebrafish have implicated these proteins in cardiovascular development. How loss of this signaling pathway leads to these diverse cardiovascular defects, however, has not been clear. Our studies of the expression and function of HEG1 and CCM2 support a mechanism in which HEG1 receptor signaling through CCM proteins is required to regulate endothelial cell-cell association during formation of the cardiovascular system, and for its integrity thereafter. The identification of endothelial junction defects in the dilated hearts and vessels of deficient fish and mice identical to those in human CCMs suggests that this pathway regulates vertebrate cardiovascular development and human CCM pathogenesis through control of endothelial cell association.

Several lines of evidence suggest that the vascular defects observed in fish, mice and humans lacking HEG1 and CCM proteins reflect the loss of an endothelial cell signaling pathway. Although CCM gene expression is relatively low and not vascular-specific, HEG1 expression is detected specifically in vascular tissues and is restricted to endothelial cells at the stages at which deficient mouse and fish embryos first develop cardiovascular defects. The vascular defects observed in E9 $Heg1^{-/-};Ccm2^{lacZ/+}$ and $Ccm2^{lacZ/lacZ}$ mouse embryos and 48 hpf morphant zebrafish embryos lacking heg or ccm2 arise prior to the appearance of other vascular cell types such as pericytes or smooth muscle cells in which HEG1 receptors might function to indirectly regulate endothelial cell function. Consistent with these observations, mosaic analysis in zebrafish embryos has suggested that krit1 functions cell autonomously during cardiovascular development 24. Finally, CCM2 knockdown endothelial cells are defective in the formation of lumenized tubes and biochemical studies demonstrate that HEG1 receptors couple to CCM proteins such as CCM2 primarily through the KRIT1 protein. These findings strongly support a conserved cell autonomous

mechanism in which HEG1 receptors signal through CCM proteins to regulate endothelial cells during the formation and function of cardiovascular organs.

How are non-patent branchial arch arteries in early deficient mouse and fish embryos, the diverse cardiovascular integrity defects in older HEG1-deficient mice, and human cerebral cavernous malformations linked? Their common ultrastructural defects in endothelial junctions suggest that all of these phenotypes may be explained by varying degrees of loss of endothelial cell-cell association. In our studies the most severe loss of function confers the cardiovascular defects observed in 48 hpf morphant zebrafish embryos and E9 *Heg1*$^{-/-}$;*Ccm2*$^{lacZ/+}$ and *Ccm2*$^{lacZ/lacZ}$ mouse embryos. In these animals the differentiation and proliferation of early endothelial cells and their migration to sites of vessel formation (i.e. vessel patterning) are undisturbed and we also find normal migration of CCM2-deficient HUVEC *ex vivo* (Supp. Fig. 7), but endothelial cell assembly into a lumenized, patent circulatory system is blocked. Recent studies in zebrafish suggest that patent vessels may arise either through the coalescence of vacuoles in single endothelial cells22, i.e. an intra-endothelial cell mechanism, or through the circumferential arrangement of endothelial cells that are connected by cell-cell junctions21,23, i.e. an inter-endothelial cell mechanism. Our finding that endothelial cell vacuolization and lumenization are preserved in the ISVs of zebrafish embryos lacking this pathway is most consistent with an inter-endothelial defect in cell-cell association. The integrity defects observed in the heart, blood vessels and lymphatic vessels of HEG1-deficient mice also support a mechanism of impaired endothelial cell-cell association. The dilated, leaky lymphatic vessels of HEG1-deficient mice reproduce many of the key structural and functional defects observed in human CCMs and in heg-deficient fish hearts, including shortened endothelial cell junctions, abnormal coverage of endothelial cells by adjacent cell types such as pericytes or cardiomyocytes, and vessel leak and rupture. In addition, we observe dilated lymphatic vessels in *Heg1*$^{+/-}$;*Ccm2*$^{+/lacz}$ animals but not in *Heg1*$^{+/-}$ or *Ccm2*$^{+/lacz}$ animals (data not shown), a result consistent with a genetic link between HEG1 and CCM2 in the formation of CCM-like dilated vessels as well as in early vessel formation in embryos. Finally, KRIT1 has recently been found to localize at and functionally regulate endothelial cell junctions 17, and we find that heterologously expressed HEG1-YFP receptors similarly co-localize with beta-catenin at endothelial junctions (Supp. Fig. 10). Thus a unified mechanism for these diverse vertebrate phenotypes is one in which HEG1 signaling through CCM proteins is required for endothelial cells to associate with each other to create and maintain vertebrate cardiovascular organs.

A final question with important therapeutic implications is whether and how these studies advance our understanding of human CCM pathogenesis. While the molecular and genetic pathways that underlie embryonic cardiovascular development and adult cardiovascular disease are frequently postulated to be conserved, such links are often tenuous. It is therefore remarkable that our studies of HEG1-CCM signaling in developing mice and fish support a linear conservation of the role of this pathway in both development and disease. Our findings suggest that the primary role of HEG1-CCM signaling is to control the association of endothelial cells to create and maintain cardiovascular structures. Thus CCMs are predicted to be a disease of defective endothelial association, and agents that positively regulate endothelial junction formation might provide a means of stabilizing human CCMs

and/or preventing their de novo formation. Alternatively, activation of HEG1-CCM signaling might provide a means of treating vascular diseases characterized by vascular leak or defective vessel integrity, such as sepsis. Studies to define better the components and *in vivo* role of this novel signaling pathway may therefore identify new strategies for treating inherited and acquired vascular diseases.

Supplementary Material

Refer to Web version on PubMed Central for supplementary material.

Acknowledgements

We thank C. Bertozzi, C. Chen, A. Granger, J. Lee, P. Mericko, A. Schmaier, E. Sebzda, N. Shanbhag and S. Sweeney for valuable insights. We thank M. Pack and J. He for assistance with zebrafish studies. We thank R. Meade for preparation of the electron microscopy samples and T. Branson for animal husbandry. This work was supported by NIH grants T32 HL07439 (BK), HL078784 and AR27214 (MG), HL62454 (JK) and HL075380 and HL095326 (MLK).

Appendix

Methods

Mice

SV/129 ES cells heterozygous for the *Heg1* allele were generated by deletion of exon 1 using recombineering-based gene-targeting techniques and microinjected into C57Bl/6 blastocysts. F1 generation $Heg1^{+/-}$ animals (50% 129;50% C57Bl/6) were intercrossed and phenotypic analysis was conducted on $Heg1^{-/-}$ and wild type littermates. $Heg1^{+/-}$ animals in >95% C57Bl/6 were generated through backcrossing. $Ccm2^{lacZ/+}$ animals were generated from 129P2 embryonic stem cells in which an IRES-ßGeo cassette was inserted into *Ccm2* exon 6 using a retroviral gene trap (Bay Genomics clone RRG05113). Tie2-Cre transgenic animals and ROSA26R mice were obtained from Jackson Research Laboratories (Bar Harbor, ME). Unless otherwise specified, all mice were maintained on a mixed genetic background. Animal protocols were approved by the University of Pennsylvania Institutional Animal Care and Use Committee. Genotyping primer sequences are available in Supplemental Methods.

In situ hybridization and immunostaining

Primer sequences used to generate *Heg1* and *Ccm2 in situ* probes are available in Supplemental Methods. Radioactive in situ hybridization, immunostaining, and TUNEL-staining were performed on paraformaldehyde-fixed, paraffin-embedded sections. Detailed protocols are available at: http://www.med.upenn.edu/mcrc/histology_core/. Antibodies used for immunostaining of tissue sections were: rabbit monoclonal antibody to Ki67, 1:250 (Vector Laboratories); 1A4 mouse monoclonal antibody to α-SMA, 1:100 (Sigma); rabbit polyclonal antibody to LYVE1 25, 1:2000; mouse monoclonal antibody to beta-catenin, 1:100 (BD Transduction); rat monoclonal antibody to Flk1, 1:50 (PharMingen); and rabbit polyclonal antibody to claudin-5, 1:50 (Zymed).

Zebrafish studies

TLF wild type and *Tg(fli1a:EGFP)*^{y1} 26, *Tg(kdr:EGFP)* 27, *Tg(fli1a:EGFP-cdc42)*^{y48} 22, *ccm2*^{hi296aTg} 28 mutant zebrafish lines were maintained and bred. Antisense morpholino oligonucleotides (Gene Tools) that interfere with the splicing of *ccm2* (*ccm2* MO) and *heg* (*heg* MO)11,12 were injected into the yolk of one-cell stage embryos at a dose of 5 ng. To rescue the "big heart" phenotype caused by *ccm2* MO, the one-cell stage embryos were first injected with *ccm2* MO at 5 ng dosage, and then half of the *ccm2* MO injected embryos were injected with 100 pg *ccm2* or *ccm2 L197R* cRNA. Microangiography of zebrafish embryos was performed as previously described 29. Red fluorescent (580/605) 0.02 μm carboxylate-modified FluoSphere beads (Invitrogen) or 10 mg ml^{-1} 70 kDa FITC Dextran (Sigma) were injected into the sinus venosus of 48 hpf zebrafish embryos. Embryos were mounted laterally in 2% methylcellulose and the images were acquired using Olympus MVX10 microscope.

Immunoprecipitation and immunoblotting

Full-length HEG1 without endogenous signal peptide (AA 38-1313) and C-terminally truncated HEG1 (AA 38-1207) were subcloned into pcDNA3.1 with a human IL-1 signal peptide, an N-terminal FLAG epitope, and a C-terminal v5 epitope (see Supplemental Figure 1b). His_6-recombinant HEG1 cytoplasmic-tail containing an *in vivo* biotinylation peptide tag at the amino-terminus was cloned into pET15b as previously described with integrin cytoplasmic-tail model proteins 30. Tail proteins were expressed and purified from *E. coli* 31.

For co-immunoprecipitation studies, FLAG-tagged full-length and truncated HEG1 and HA-tagged CCM2 were transfected into HEK293T cells. After 48 h, cells were incubated for 10 min in lysis buffer (50 mM TRIS HCl, 150 mM NaCl, 25 mM EDTA, 1% NP-40, 0.5% sodium deoxycholate, pH 8, containing PhosStop (Roche) and Complete protease inhibitor (Roche)), drawn through a 25-gauge needle and cleared by centrifugation. FLAG immunoprecipitations were performed with 2 μg ml^{-1} M2 antibody to FLAG (Sigma) and CCM2 immunoprecipitations performed with #2055 polyclonal antibody to CCM2 for >2 h and then with Protein G agarose (Invitrogen) for 1 h. Proteins were detected using the following antibodies: M2 mouse monoclonal antibody to FLAG, 1:500 (Sigma), mouse monoclonal antibody to HA, 1:2000 (Abcam), HRP-conjugated goat antibody to mouse IgG, 1:5000 (Jackson ImmunoResearch).

For affinity matrix pulldowns, HEK293T and CHO cells were transfected with Myc-KRIT1, HA-CCM2, FLAG-krit1, HA-ccm2, HA-ccm2 L197R and FLAG-CCM2. Cells were incubated for 10 minutes in lysis buffer (25 mM HEPES (pH 7.4), 100 mM NaCl, 0.5% NP-40, and Complete protease inhibitor (Roche)). After clarification, 350 mg lysate was incubated with 10 mg immobilized HEG1 tail overnight. Proteins were detected using the following antibodies: M2 mouse monoclonal antibody to FLAG, 1:2000 (Sigma), mouse monoclonal antibody to Myc, 1:2000 (Abcam), mouse monoclonal antibody to HA, 1:2000 (Abcam), polyclonal antibody to KRIT-1 6832, 1:1000 17, HRP-conjugated goat antibody to mouse IgG, 1:5000 (Jackson ImmunoResearch), HRP-conjugated donkey antibody to rabbit IgG, 1:5000 (Jackson ImmunoResearch). All steps were performed at 4 °C.

Electron microscopy and cell-cell junction quantitation

Neonatal mouse gut mesentery, 48 hpf zebrafish embryos and E9.5 mouse embryos were fixed overnight, embedded in Polybed 812 (Polysciences Inc.), sectioned, stained and examined with a JEOL 1010 electron microscope fitted with a Hamamatsu digital camera. All identifiable endocardial cell-cell junctions from *6 Heg1*$^{+/+}$ and 5 *Heg1*$^{-/-}$ lymphatic vessel cross-sections (66 and 123 junctions, respectively) were imaged and junction lengths were quantitated using ImageJ. Endothelial cell-cell junctions from 3 control and 4 *ccm2* MO zebrafish atria cross-sections (88 and 107 junctions, respectively) and 4 *Ccm2*$^{+/+}$ and 6 *Ccm2*$^{lacz/lacz}$ dorsal aorta cross-sections (128 and 107 junctions, respectively) were imaged and quantitated as above. Junctions were ordered by length and the mean junction length for each tercile was determined. The percentage of junctions less than 1000 nm, between 1000 and 2500 nm, and greater than 2500 nm was also calculated. Lastly, the overall mean junction length was calculated from the mean junction lengths for each heart or vessel cross-section.

Statistics

P values were calculated using an unpaired 2-tailed Student's t-test or Chi Square analysis as indicated.

References

1. Rigamonti D, et al. Cerebral cavernous malformations. Incidence and familial occurrence. N Engl J Med. 1988; 319:343–7. [PubMed: 3393196]
2. Revencu N, Vikkula M. Cerebral cavernous malformation: new molecular and clinical insights. J Med Genet. 2006; 43:716–21. [PubMed: 16571644]
3. Sahoo T, et al. Mutations in the gene encoding KRIT1, a Krev-1/rap1a binding protein, cause cerebral cavernous malformations (CCM1). Hum Mol Genet. 1999; 8:2325–33. [PubMed: 10545614]
4. Eerola I, et al. KRIT1 is mutated in hyperkeratotic cutaneous capillary-venous malformation associated with cerebral capillary malformation. Hum Mol Genet. 2000; 9:1351–5. [PubMed: 10814716]
5. Liquori CL, et al. Mutations in a gene encoding a novel protein containing a phosphotyrosine-binding domain cause type 2 cerebral cavernous malformations. Am J Hum Genet. 2003; 73:1459–64. [PubMed: 14624391]
6. Denier C, et al. Mutations within the MGC4607 gene cause cerebral cavernous malformations. Am J Hum Genet. 2004; 74:326–37. [PubMed: 14740320]
7. Bergametti F, et al. Mutations within the programmed cell death 10 gene cause cerebral cavernous malformations. Am J Hum Genet. 2005; 76:42–51. [PubMed: 15543491]
8. Zawistowski JS, et al. CCM1 and CCM2 protein interactions in cell signaling: implications for cerebral cavernous malformations pathogenesis. Hum Mol Genet. 2005; 14:2521–31. [PubMed: 16037064]
9. Voss K, et al. CCM3 interacts with CCM2 indicating common pathogenesis for cerebral cavernous malformations. Neurogenetics. 2007
10. Zhang J, Rigamonti D, Dietz HC, Clatterbuck RE. Interaction between krit1 and malcavernin: implications for the pathogenesis of cerebral cavernous malformations. Neurosurgery. 2007; 60:353–9. discussion 359. [PubMed: 17290187]
11. Mably JD, Mohideen MA, Burns CG, Chen JN, Fishman MC. heart of glass regulates the concentric growth of the heart in zebrafish. Curr Biol. 2003; 13:2138–47. [PubMed: 14680629]
12. Mably JD, et al. santa and valentine pattern concentric growth of cardiac myocardium in the zebrafish. Development. 2006; 133:3139–46. [PubMed: 16873582]

13. Plummer NW, et al. Neuronal expression of the Ccm2 gene in a new mouse model of cerebral cavernous malformations. Mamm Genome. 2006; 17:119–28. [PubMed: 16465592]
14. Wong JH, Awad IA, Kim JH. Ultrastructural pathological features of cerebrovascular malformations: a preliminary report. Neurosurgery. 2000; 46:1454–9. [PubMed: 10834648]
15. Clatterbuck RE, Eberhart CG, Crain BJ, Rigamonti D. Ultrastructural and immunocytochemical evidence that an incompetent blood-brain barrier is related to the pathophysiology of cavernous malformations. J Neurol Neurosurg Psychiatry. 2001; 71:188–92. [PubMed: 11459890]
16. Tu J, Stoodley MA, Morgan MK, Storer KP. Ultrastructural characteristics of hemorrhagic, nonhemorrhagic, and recurrent cavernous malformations. J Neurosurg. 2005; 103:903–9. [PubMed: 16304995]
17. Glading A, Han J, Stockton RA, Ginsberg MH. KRIT-1/CCM1 is a Rap1 effector that regulates endothelial cell cell junctions. J Cell Biol. 2007; 179:247–54. [PubMed: 17954608]
18. Whitehead KJ, Plummer NW, Adams JA, Marchuk DA, Li DY. Ccm1 is required for arterial morphogenesis: implications for the etiology of human cavernous malformations. Development. 2004; 131:1437–48. [PubMed: 14993192]
19. Nakatsu MN, et al. Angiogenic sprouting and capillary lumen formation modeled by human umbilical vein endothelial cells (HUVEC) in fibrin gels: the role of fibroblasts and Angiopoietin-1. Microvasc Res. 2003; 66:102–12. [PubMed: 12935768]
20. Folkman J, Haudenschild C. Angiogenesis in vitro. Nature. 1980; 288:551–6. [PubMed: 6160403]
21. Jin SW, Beis D, Mitchell T, Chen JN, Stainier DY. Cellular and molecular analyses of vascular tube and lumen formation in zebrafish. Development. 2005; 132:5199–209. [PubMed: 16251212]
22. Kamei M, et al. Endothelial tubes assemble from intracellular vacuoles in vivo. Nature. 2006; 442:453–6. [PubMed: 16799567]
23. Blum Y, et al. Complex cell rearrangements during intersegmental vessel sprouting and vessel fusion in the zebrafish embryo. Dev Biol. 2008; 316:312–22. [PubMed: 18342303]
24. Hogan BM, Bussmann J, Wolburg H, Schulte-Merker S. ccm1 cell autonomously regulates endothelial cellular morphogenesis and vascular tubulogenesis in zebrafish. Hum Mol Genet. 2008; 17:2424–32. [PubMed: 18469344]
25. Sebzda E, et al. Syk and Slp-76 mutant mice reveal a cell-autonomous hematopoietic cell contribution to vascular development. Dev Cell. 2006; 11:349–61. [PubMed: 16950126]
26. Lawson ND, Weinstein BM. In vivo imaging of embryonic vascular development using transgenic zebrafish. Dev Biol. 2002; 248:307–18. [PubMed: 12167406]
27. Jin SW, et al. A transgene-assisted genetic screen identifies essential regulators of vascular development in vertebrate embryos. Dev Biol. 2007; 307:29–42. [PubMed: 17531218]
28. Amsterdam A, Hopkins N. Retroviral-mediated insertional mutagenesis in zebrafish. Methods Cell Biol. 2004; 77:3–20. [PubMed: 15602903]
29. Weinstein BM, Stemple DL, Driever W, Fishman MC. Gridlock, a localized heritable vascular patterning defect in the zebrafish. Nat Med. 1995; 1:1143–7. [PubMed: 7584985]
30. Lim CJ, et al. Alpha4 integrins are type I cAMP-dependent protein kinase-anchoring proteins. Nat Cell Biol. 2007; 9:415–21. [PubMed: 17369818]
31. Pfaff M, Liu S, Erle DJ, Ginsberg MH. Integrin beta cytoplasmic domains differentially bind to cytoskeletal proteins. J Biol Chem. 1998; 273:6104–9. [PubMed: 9497328]

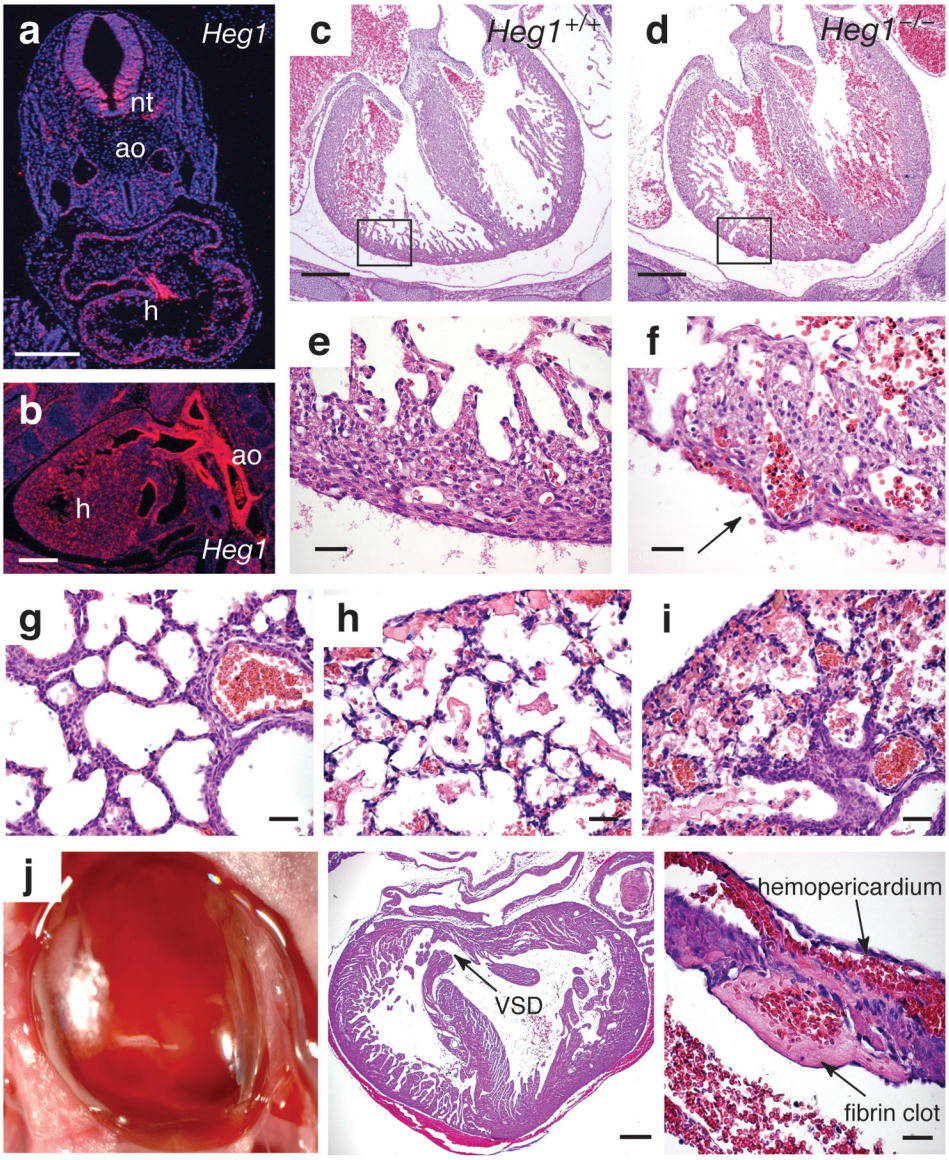

Figure 1. Lethal cardiac and blood vessel integrity defects in HEG1-deficient embryos and neonates

(**a-b**) *Heg1* is selectively expressed in the developing cardiovascular system. Radioactive in situ hybridization reveals *Heg1* expression in the vascular endothelium, cardiac endocardium and neural tube at E10.5 (**a**). By E14.5 *Heg1* is expressed in both endothelial and smooth muscle cells in major arteries (**b**). (**c-f**) E15 *Heg1*$^{-/-}$ embryos exhibit deep invaginations of the ventricular chamber into the compact zone of the ventricular wall and into the septum, often associated with the presence of blood between the epicardial and myocardial cell layers of the heart (arrow; **e,f** show boxed regions for **c,d**). (**g-i**) Pulmonary hemorrhage in *Heg1*$^{-/-}$ neonates (**h,i**) but not in *Heg1*$^{+/+}$ littermates (**g**) was manifest by the presence of erythrocytes and fibrin in alveolar air spaces. (**j**) Cardiac rupture in P4 *Heg1*$^{-/-}$ neonate. Hemopericardium (left, middle panels) associated with cardiac rupture and formation of a transmural thrombus (right panel) was observed in *Heg1*$^{-/-}$ animals. VSD,

ventricular septal defect. Scale bars in **a-d** and **j** (middle panel), 200 μm, **e-i** and **j** (right panel), 20 μm.

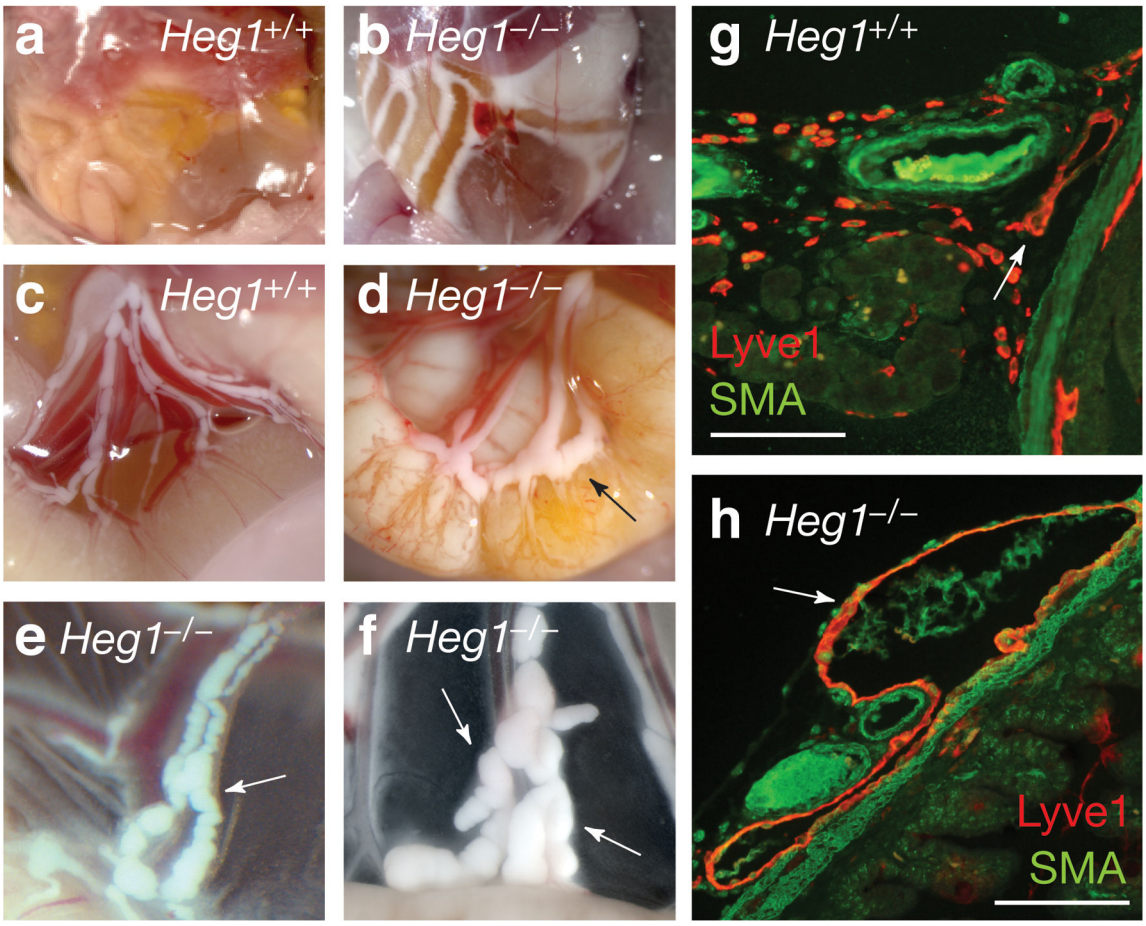

Figure 2. Lymphatic vessel dilatation and leak in *Heg1*$^{-/-}$ neonates

(a,b) HEG1-deficient neonates exhibit chylous ascites manifest by the accumulation of white chyle in the peritoneal space. (**c-f**) Lymphatic malformations in *Heg1*$^{-/-}$ animals. Neonatal mesenteric lymphatic vessels of *Heg1*$^{-/-}$ animals are dilated (arrows) and leak chyle into the intestinal wall as well as the peritoneum. Anti-LYVE1 immunostaining confirms the lymphatic identity of the dilated mesenteric vessels (arrows) (**g,h**). SMA, α-smooth muscle actin. Scale bars, 100 μm.

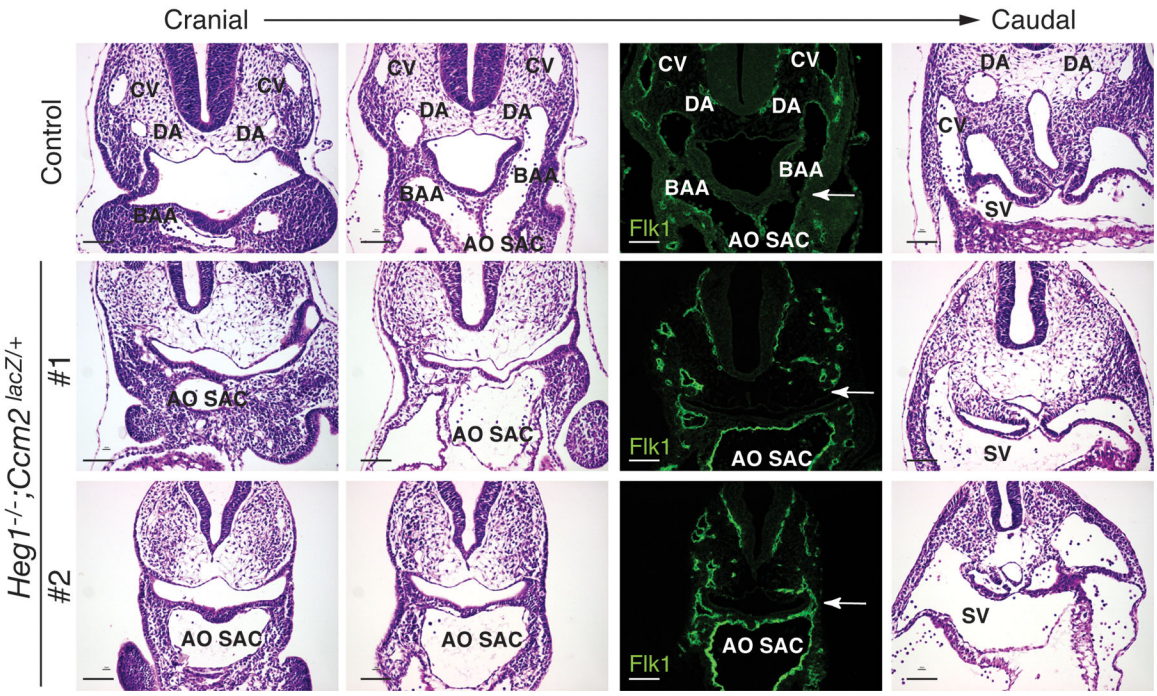

Figure 3. *Heg1*$^{-/-}$;*Ccm2*$^{+/lacZ}$ embryos fail to establish a patent blood vascular network

Transverse sections of E9 *Heg1*$^{+/-}$;*Ccm2*$^{+/+}$ (control) and two *Heg1*$^{-/-}$;*Ccm2*$^{+/lacZ}$ embryos at three levels are shown. H-E staining reveals the presence of blood-filled dorsal aortae (DA), cardinal veins (CV) and branchial arch arteries (BAA) of normal caliber in the *Heg1*$^{+/-}$;*Ccm2*$^{+/+}$ control embryo (top) but not in *Heg1*$^{-/-}$;*Ccm2*$^{+/lacZ}$ littermates (below). Anti-Flk1 staining of adjacent sections at the level of the first two branchial arch arteries is shown (middle). Flk1+ endothelial cells are present at the sites of the dorsal aortae, cardinal veins and branchial arch arteries (arrows) in *Heg1*$^{-/-}$;*Ccm2*$^{+/lacZ}$ embryos but these cells do not form vessels of normal caliber with patent lumens. SV, sinus venosus. Scale bars, 50 μm.

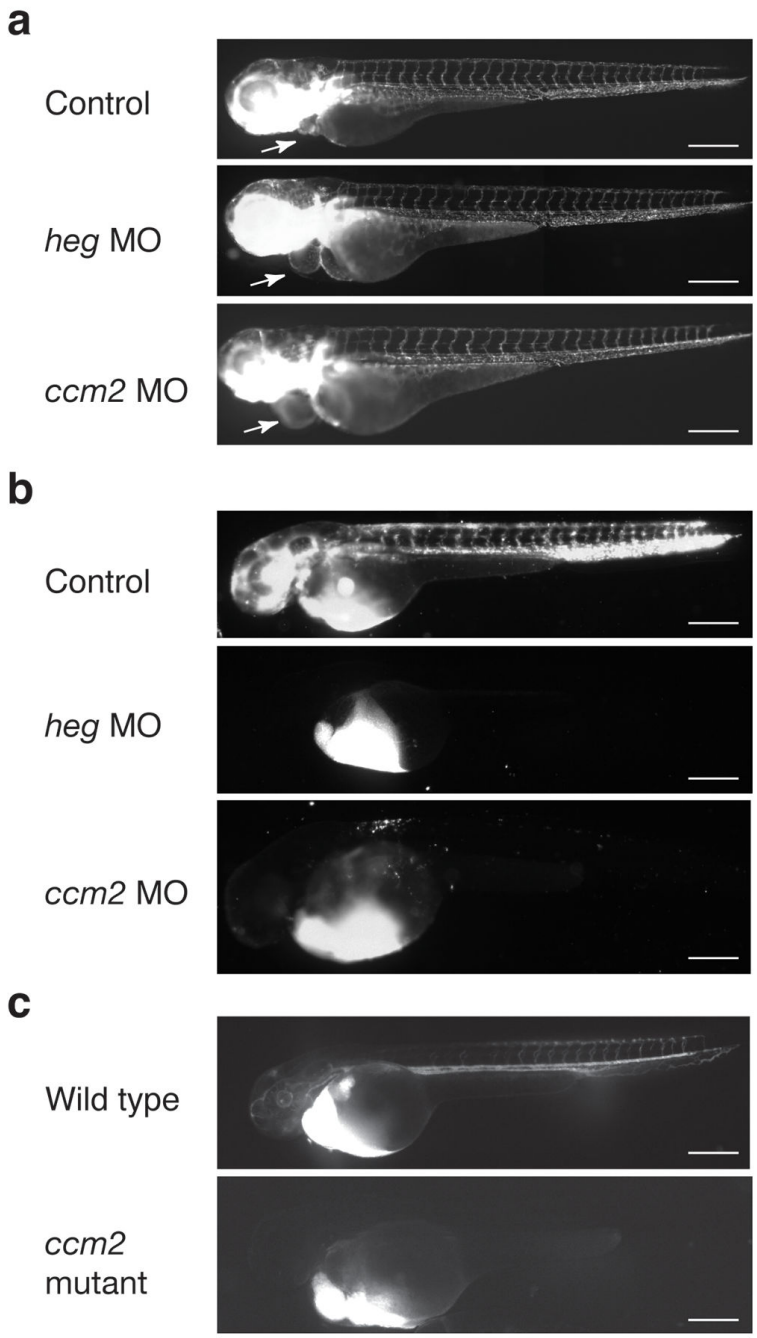

Figure 4. The endothelial cells of zebrafish lacking heg or ccm2 form vessels that are normally patterned but not patent

(**a**) Fli1-GFP transgenic *heg* and *ccm2* morphant embryos exhibit dilated hearts (arrows) and normal vascular patterning. (**b**) Angiography reveals a proximal circulatory block in *heg* and *ccm2* morphant zebrafish. Fluorescent microspheres distribute throughout the vasculature of control but not *heg* or *ccm2* morphant fish following venous injection. (**c**) FITC-dextran distributes throughout the vasculature in wild type but not *ccm2* mutant fish following venous injection. Scale bars, 250 μm.

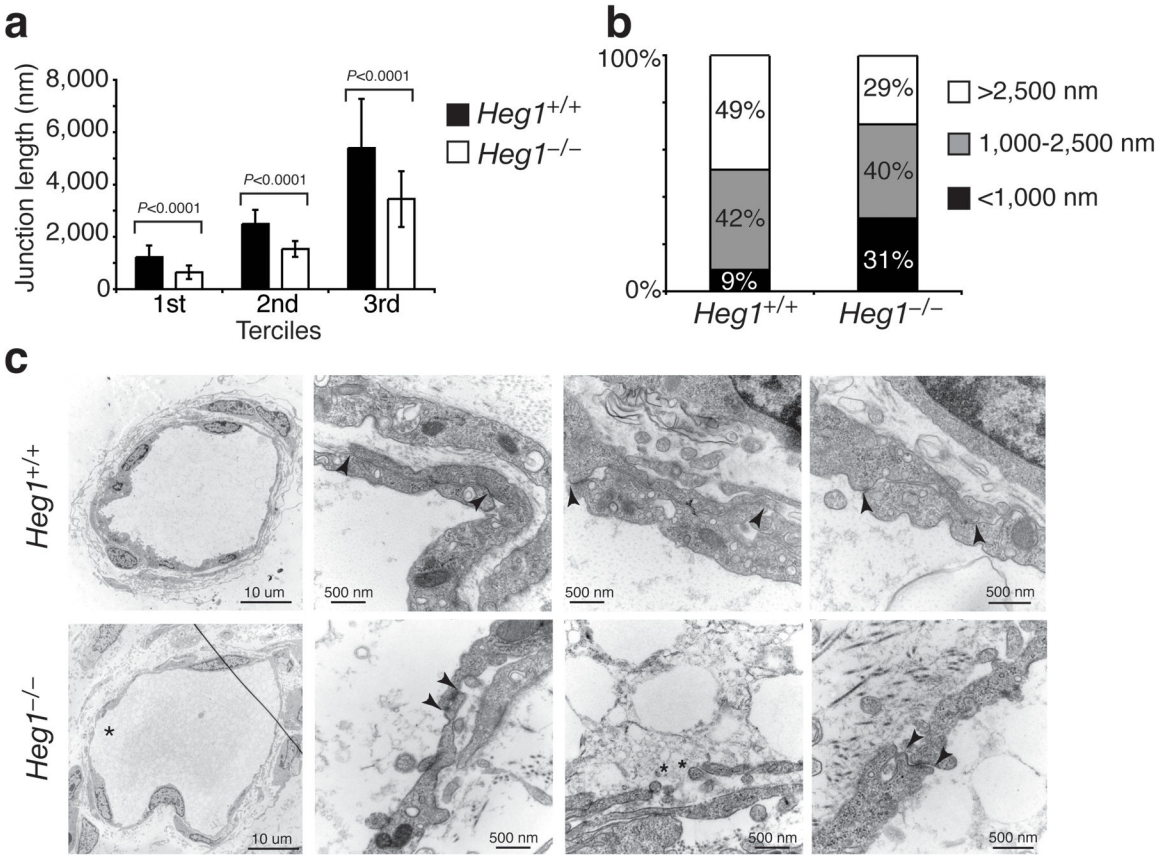

Figure 5. HEG1 is required to form normal endothelial junctions *in vivo*

(**a-c**) Dilated mesenteric lymphatic vessels in *Heg1*$^{-/-}$ mice have severely shortened endothelial junctions and gaps between endothelial cells. (**a**) The mean and standard deviation of endothelial cell junction lengths in *Heg1*$^{+/+}$ and *Heg1*$^{-/-}$ lymphatic vessels are shown, divided into terciles (1st, shortest third of junctions in each group; 2nd, middle third of junctions in each group; 3rd, longest third of junctions in each group). N = 66 *Heg1*$^{+/+}$ junctions and 123 *Heg1*$^{-/-}$ junctions. (**b**) The percent of endothelial junctions that were less than 1,000 nm (black), 1,000-2,500 nm (grey), and over 2,500 nm (white) in the indicated groups is shown. (**c**) Representative low magnification (far left) and high magnification images of endothelial cells are shown. Asterisks indicate sites of endothelial gaps, normally not present in collecting mesenteric lymphatics, and arrowheads indicate endothelial junction limits. Note the presence of endothelial gaps in *Heg1*$^{-/-}$ but not *Heg1*$^{+/+}$ vessels.

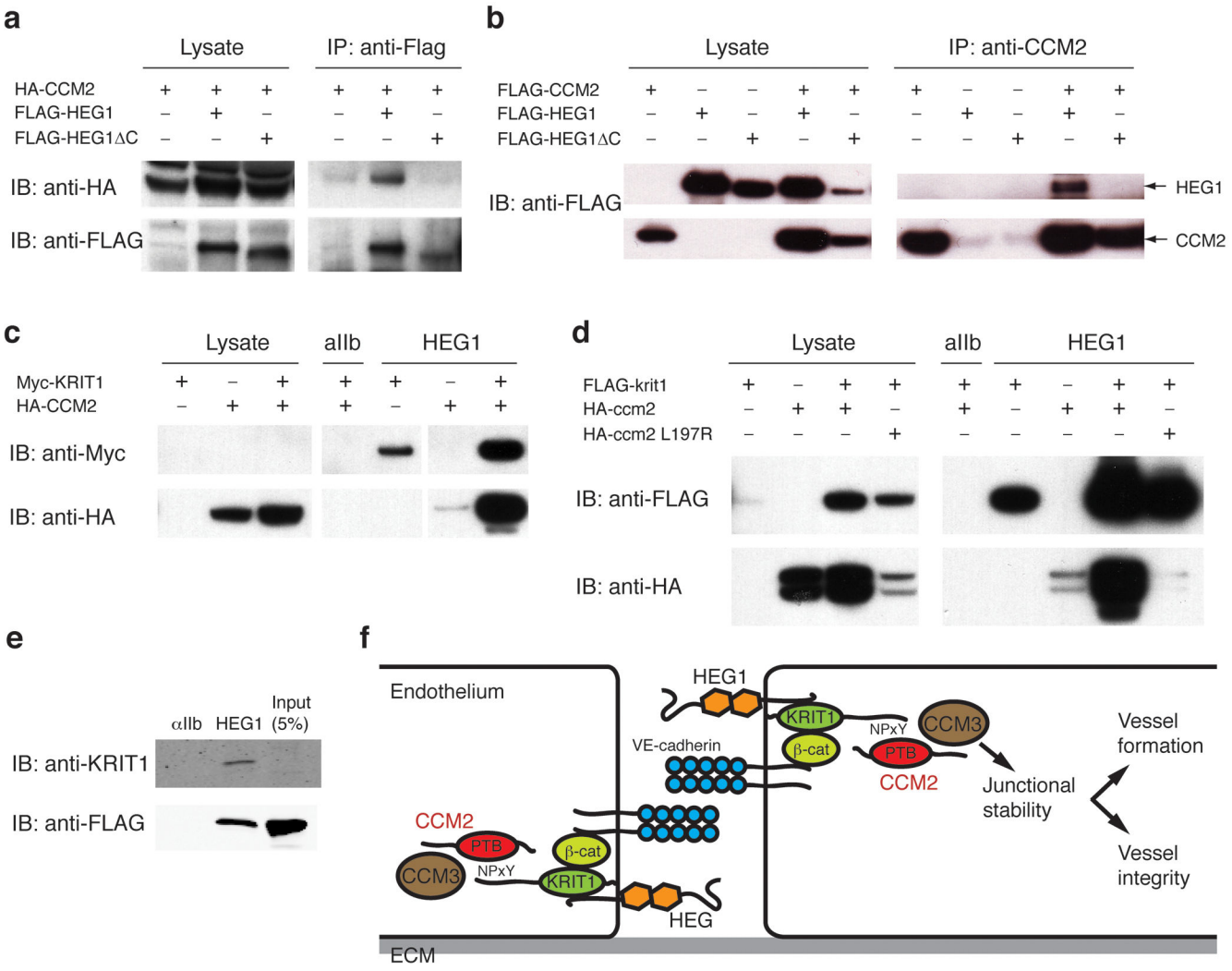

Figure 6. HEG1 receptor intracellular tails associate with CCM2 through KRIT1

(**a,b**) Co-immunoprecipitation of HEG1 and CCM2 requires the HEG1 receptor intracellular tail. HA-CCM2 or FLAG-CCM2 and FLAG-HEG1 or FLAG-HEG1ΔC, a mutant lacking the terminal 106 amino acids of the HEG1 carboxy tail, were coexpressed in HEK293T cells and immunoprecipitations performed using anti-FLAG (**a**) and anti-CCM2 antibodies (**b**). (**c**) HEG1 intracellular tails interact with KRIT1 and CCM2. HA-tagged mouse CCM2 and Myc-tagged mouse KRIT1 were expressed in HEK293 cells and pulldowns performed with affinity matrices containing the intracellular tail of either the aIIb integrin subunit (aIIb) or the HEG1 receptor (HEG1). Note that the HEG1 receptor tail efficiently pulls down KRIT1 in the absence of CCM2 but not vice versa. (**d**) HEG1 interacts with CCM2 through KRIT1. FLAG-tagged zebrafish krit1, HA-tagged zebrafish ccm2 and HA-tagged zebrafish ccm2 L197R were expressed in HEK293 cells and pulldowns performed using aIIb or HEG1 tail affinity matrices as in **c**. Note that ccm2 L197R does not associate with the HEG1 tail (far right lane). (**e**) The HEG1 receptor tail efficiently binds endogenous KRIT1. Pulldowns using aIIb or HEG1 tail affinity matrices were performed using cell lysate from CHO cells transfected with FLAG-tagged CCM2. Endogenous KRIT1 was detected with anti-KRIT1

monoclonal antibody (top) and heterologous CCM2 detected with anti-FLAG monoclonal antibody (bottom). The far right lane shows immunoblotting of cell lysate equivalent to 5% of the input for the pull downs. (**f**) Molecular model of HEG1-CCM signaling at endothelial cell junctions. Shown are HEG1 receptors coupling to KRIT1 and CCM2 via HEG1 tail-KRIT1 and KRIT1-CCM2 interactions, respectively. KRIT1 also interacts with the junctional proteins VE-cadherin and beta-catenin, and HEG1-CCM signaling is proposed to regulate junction formation and function.